Convergence Analysis of LU scheme for Euler/Navier-Stokes Equations on Unstructured Meshes

J. S. Kim [1], O. J. Kwon [2]
1.Doctoral Candidate, Department of Aerospace Engineering
2. Associate Professor, Department of Aerospace Engineering

Abstract

A comprehensive study has been made for the investigation of the convergence characteristics of the LU scheme for the Euler equations using Von Neumann stability analysis. The stability results indicate that the convergence rate is governed by a specific parameter combination. Based on this insight, it is shown that the LU scheme will not suffer convergence deterioration at any grid aspect ratios if the local time step is defined using an appropriate parameter combination. The numerical results demonstrate that this time step definition gives uniform convergence for grid aspect ratios from one to million.

Keyword: *LU scheme, Von Neumann stability analysis, Euler equations, Unstructured meshes*

1. Introduction

Most of implicit schemes for computational fluid dynamics(CFD) rely on approximate inversion methods for solving the linear system of equations resulting from the local time linearization of the governing equations. Currently, several popular approximate inversion methods are available including the alternating-direction implicit(ADI) scheme, the line Gauss—Seidel(LGS) scheme, and the lower-upper(LU) scheme. The LU scheme was initially proposed by Jameson and Turkel[1] and has been widely used over past couple of decades. This scheme is particularly efficient for unstructured mesh topologies because it does not require spatial coordinate direction splitting[2, 3].

There are five independent CFD parameters for the Euler equations for which govern the convergence characteristics of the LU scheme: grid aspect ratio, flow angle, Mach number, CFL number, and number of sub-iteration. Several researches have been made to investigate the characteristics of the LU scheme, but for only one or two parameters[4, 5]. In the present study, the characteristics is assessed for all parameters except Mach number using a Von Neumann stability analysis. Verification is made for simple free stream flow with a point disturbance.

2. Numerical Algorithm

The governing two-dimensional Euler equations are spatially discretized by using a node-based finite-volume method. The control volume is constructed from median dual cells surrounding each node[6]. The convective flux vector is computed using the flux-difference splitting scheme of Roe. For a high-order scheme, estimation of the primitive variables at each control volume face is achieved by interpolating the solution around the central node by using a Taylor series expansion. The solution gradient in Taylor series expansion is calculated by using an unweighted least-squares procedure[6]. This high-order scheme corresponds with a second-order upwind biased MUSCL scheme in structured grid[7].

The discretized governing equation can be factorized into the following LU form[5]:

$$(D+T_1)D^{-1}(D+T_2)\Delta Q = -R_i^n \tag{1}$$

Here, D represents the diagonal part of the linear system of equations, and T_1 and T_2 represent the lower and upper parts, respectively. It is customary with the LU scheme to perform several sub-

iterations at each time step. The corresponding multi-sweep LU scheme may be expressed as follows[5]:

$$(D+T_1)D^{-1}(D+T_2)(Q^{k+1}-Q^k)=-R_i^n-(D+T_1+T_2)(Q^k-Q^n) \tag{2}$$

where *n* and *k* represent sub-iteration and outer-iteration counter, respectively.

3. Stability Analysis

The multi-sweep LU scheme in equation (2) may be rearranged as follows to investigate the LU scheme systematically:

$$(D+T_1+T_2)(Q^{k+1}-Q^n)-T_1D^{-1}T_2(Q^{k+1}-Q^k)=-R_i^n \tag{3}$$

In the above equation, the first term in left hand side correspond with the direct inversion scheme. Also, the second term represents the approximate factorization(AF) error for the LU scheme. Therefore, for the complete analysis of the LU scheme, the contribution from each of the direct inversion and the AF error needs to be examined separately.

3.1 Direct Inversion Scheme

3.1.1 Scalar convection equation

Before the analysis for the Euler equations, a scalar model equation of the hyperbolic type is considered for the simplicity. The equation studied here is

$$\frac{\partial u}{\partial t}+a\frac{\partial u}{\partial x}+b\frac{\partial u}{\partial y}=0 \tag{4}$$

where *a* and *b* are positive and negative values, respectively. By taking different signs for the convection speeds in equation (4), the equation can be used meaningfully as model equation for the Euler equations with both positive and negative eigenvalues. The Von Neumann analysis for the direct inversion and second order upwind spatial accuracy schemes results in the amplification factor:

$$G=\frac{1+\frac{1}{4}\frac{CFL}{2(1+\theta AR)}\Phi}{1+\frac{CFL}{2(1+\theta AR)}\Psi} \tag{5}$$

where Φ and Ψ are defined in terms of the two spatial frequencies:

$$\begin{aligned}\Phi&=\left[(1-Cos2\phi_x)+\theta AR(1-Cos2\phi_y)\right]+\left[(-2Sin\phi_x+Sin2\phi_x)-\theta AR(-2Sin\phi_y+Sin2\phi_y)\right]I\\ \Psi&=\left[(1-Cos\phi_x)+\theta AR(1-Cos\phi_y)\right]+\left[Sin\phi_x-\theta ARSin\phi_y\right]I\end{aligned} \tag{6}$$

The *CFL* number in equation (6) are defined as follows:

$$CFL=\Delta t\frac{\oint_{\partial\Omega}|\lambda_{\max}|dl}{\Delta x\,\Delta y} \tag{7}$$

Also, the flow angle, $\theta = b/a$ and grid aspect ratio, $AR = \Delta x/\Delta y$.

The amplification factor G shows a different behavior according to the magnitude of θAR. In order to analyze this behavior, it is a convenient approach to represent the amplification factor in purely x-directional wave of $\phi_y=0$ and y-directional wave of $\phi_x=0$ separately. If the θAR has a very large value($\theta AR \gg 1$), the equation (5) can be written with some algebraic manipulation as

$$\text{Purely } x\text{-directional wave: } G = f(\frac{CFL}{AR}) \tag{8}$$

$$\text{Purely } y\text{-directional wave: } G = f(CFL) \tag{9}$$

Also, if the θAR has a very small value($\theta AR \ll 1$), it can be written as

$$\text{Purely } x\text{-directional wave: } G = f(CFL) \tag{10}$$

$$\text{Purely } y\text{-directional wave: } G = f(CFL \times AR) \tag{11}$$

The quantity of θAR can be represented as the required times for the error propagation:

$$\theta\, AR = \frac{\Delta x}{\Delta y}\frac{b}{a} = \frac{b/\Delta y}{a/\Delta x} = \frac{\Delta t_x}{\Delta t_y} \tag{12}$$

where Δt_x is the required time to move across the x-directional grid spacing, Δx , with x-directional wave speed, a, and similarly for Δt_y. If the θAR is unity, the required times for the x- and y-directions have same values. For θAR$\gg$1, the required time for the x-direction is greater than that for the y-direction, therefore it is certain that the x-directional wave is poorly damped compared with y-directional wave. Thus, it can be concluded that the damping rate for the x-directional wave dominate the overall convergence rate in the case for θAR$\gg$1:

$$G = f(\frac{CFL}{AR}) \qquad for \quad \theta >> 1/AR \tag{13}$$

If θAR$\ll$1, the y-directional wave is poorly damped, and the y-directional damping rate dominate the overall convergence rate:

$$G = f(CFL \times AR) \qquad for \quad \theta << 1/AR \tag{14}$$

In equation (13) and (14), it is shown that the convergence rate in each grid having different grid aspect ratios is governed by a single parameter, which has different form according to the magnitude of the flow angle.

The amplification factors are determined by cycling through a fixed number of each of the spatial frequencies, in this case, 101 frequencies, for each CFL number, AR, and θ. The norm of amplification factor(NAF), which is a scalar value, is calculated as

$$NAF = \left\{ \frac{1}{2\,nmax} \sum_{i=1}^{nmax} \sum_{j=1}^{nmax} \left[\left| G_{ij}\left(CFL_f, AR, \theta\right) \right| - \left| G_{ij}\left(CFL, AR, \theta\right) \right| \right]^2 \right\}^{1/2} \tag{15}$$

where CFL_f means fixed CFL number, and 10^{20} is used in the present calculation. The NAF , therefore, approaches machine zero, as CFL increases.

Fig. 1-(a) and (b) show the NAF calculated for grids with several aspect ratios for θAR$\gg$1 and θAR$\ll$1, respectively. The flow angle of 100 is used in the case for θAR$\gg$1 and the value of 0.00001 in

the case for $\theta AR \gg 1$. In Fig. 1-(a), it is shown that, for a fixed value of *CFL/AR*, the values of the NAF are similar for all aspect ratio grids in the case for large flow angle. Also, Fig. 1-(b) shows that the values of the NAF are approximately same for all aspect ratio grids for a fixed value of *CFL*×*AR* in the case for small flow angle. These behaviors correctly agree with the results of equations (13) and (14). Fig. 2 shows the details of the amplification factor for θ=100 and *CFL/AR*=10^3. It is shown that the details for each of the spatial frequencies are approximately same for all aspect ratio grids. Additional calculations for a different value of *CFL/AR* showed very similar trends, not included here. These behaviors were also observed in the cases for small flow angle. Thus, it can be said that when the NAF has similar value for each grid having different grid aspect ratios, the amplification factors show approximately same features.

The results in Figs. 1 and 2 show that the behavior of amplification factor is well predicted by the equations (13) and (14) even in details. Thus, it can be concluded that the direct inversion scheme for the scalar convection equation will not suffer convergence deterioration at any grid aspect ratios if the *CFL* number is chosen carefully using the equations (13) or (14) according to the magnitude of the flow angle.

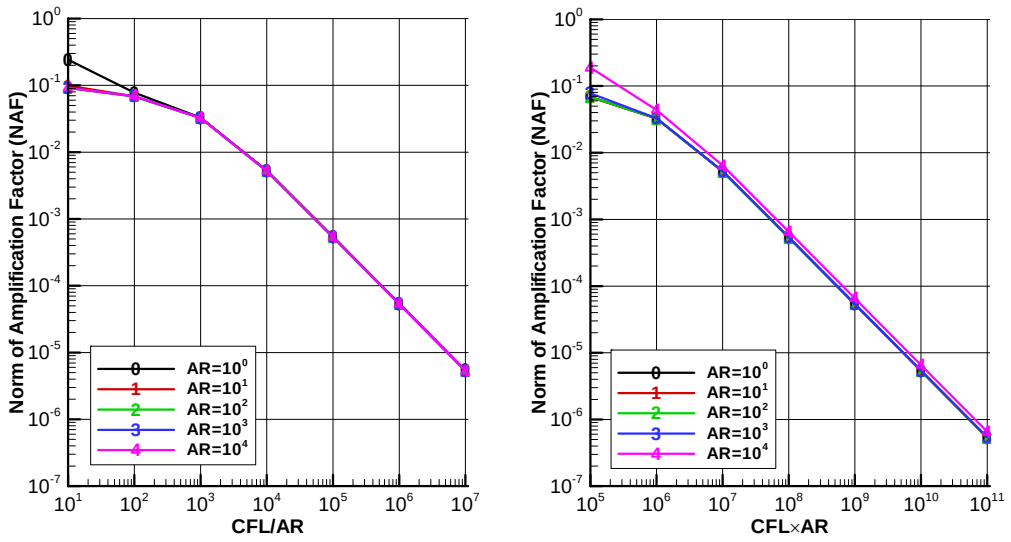

(a) $\theta AR \gg 1$ **(b) $\theta AR \gg 1$**

Fig. 1. Norms of Amplification Factor(NAF) of the scalar equation for θ=100 and θ=0.00001.

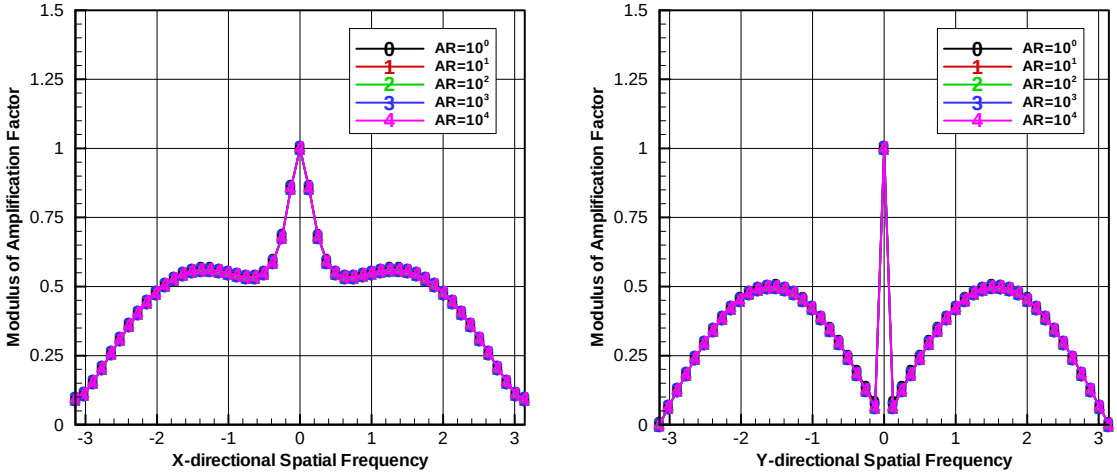

(a) Purely x-directional wave **(b) Purely y-directional wave**

Fig. 2. Modulus of amplification factor of the scalar equation for θ=100 and *CFL/AR*=10^3.

3.1.2 Euler equations

In the preceding chapter, it is seen that the amplification factor for the scalar equation show a different behavior according to the magnitude of the flow angle. The flow angle is regarded as the direction of the wave speed. For the Euler eqations, three wave speeds, u, $u+c$, and $u-c$, are present, therefore nine flow angles can be constructed. Generally, particle wave speeds, u and v, are used for the definition of flow angle for the Euler equations analyses: $\theta \equiv v/u$. However, it can be defined other flow angles such as maximum flow angle, θ_{max}, and minimum flow angle, θ_{min}, as follows:

$$\theta_{\max} = \frac{Max(v,\, v+c,\, v-c)}{Min(u,\, u+c,\, u-c)}, \quad \theta_{\min} = \frac{Min(v,\, v+c,\, v-c)}{Max(u,\, u+c,\, u-c)} \tag{16}$$

In equation (16), it may be shown that the $\theta_{max}AR$ is always less than the θAR and the $\theta_{min}AR$ is greater than the θAR. Therefore, it is obvious that, even for a very large θAR, a small flow angle can be present for any other wave speeds. Also, it is clear that a large flow angle can be presented even for a very small θ.

The NAF for the Euler equations at Mach number of 0.5 is shown in Fig. 3. Here, each figure in Fig. 3 is calculated for the same value of θAR: $\theta AR=10^{-2}$ in Fig. 3-(a) and $\theta AR=10^{0}$ in Fig. 3-(b). For the Euler equations, the meaningful results can be obtained for the same value of θAR. These figures show that the values of the NAF are approximately same for all aspect ratio grids for a fixed value of CFL/AR irrespective of flow angles. The NAF for the Euler equations does not show a different behavior according to the magnitude of flow angle as the scalar equation does. Therefore, it can be concluded that the direct inversion scheme for the Euler equations will not suffer convergence deterioration at any grid aspect ratios if the CFL number is chosen as CFL/AR for grids with different aspect ratio.

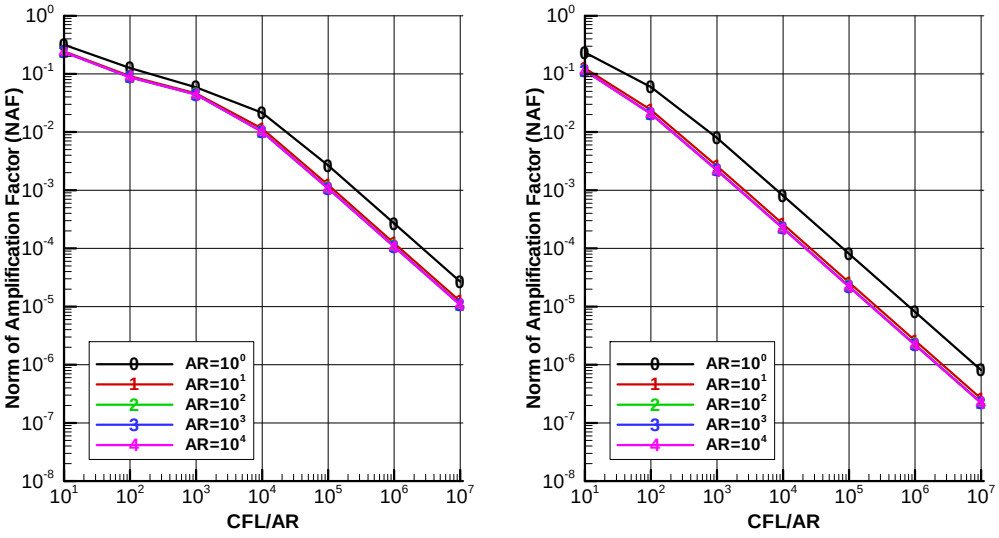

(a) θAR**=10**$^{-2}$ **(b)** θAR**=10**^{0}

Fig. 3. Norms of Amplification Factor (NAF) of the Euler equations for θAR**=10**$^{-2}$ **and** θAR**=10**^{0}**.**

3.2 AF Error

3.2.1 Scalar convection equation

The approximate factorization form of the multi-sweep LU scheme(equation (3)) shows that the AF error in this scheme is

$$AF\ error = T_1 D^{-1} T_2 \left(Q^{k+1} - Q^{k} \right) \tag{17}$$

Application of the Von Neumann stability analysis leads to

$$AF\ error = \Pi\, e^{-I\left(\phi_x - \phi_y\right)} \Delta Q_{ij} \tag{18}$$

where

$$\Pi = \frac{CFL^2}{2\left(2 + CFL\right)} \frac{\theta\, AR}{\left(1 + \theta\, AR\right)^2} \tag{19}$$

Large *CFL* number(□1) is usually used for the LU scheme, and, in this case, the equation (19) can be approximated as

$$\Pi \approx \frac{CFL}{2} \frac{\theta\, AR}{\left(1 + \theta\, AR\right)^2} \tag{20}$$

Equation (20) represents the magnitude of the AF error. Therefore, it seems reasonable to consider the behavior of equation (20) to examine the characteristics of the AF error.

The equation (20) shows a different behavior as the magnitude of of θAR as the direct inversion scheme. If the θAR has a very large value(θAR□1), the equation (20) can be written as

$$\Pi = f\left(\frac{CFL}{AR}\right) \qquad for \quad \theta >> 1/AR \tag{21}$$

Also, if the θAR has a very small value(θAR□1), it can be written as

$$\Pi = f\left(CFL \times AR\right) \qquad for \quad \theta << 1/AR \tag{22}$$

In equation (21) and (22), it is shown that the AF error in each grid having different grid aspect ratios is governed by a single parameter, which has different form according to the magnitude of the flow angle.

3.2.2 Euler equations

The AF error may be regarded conceptually as the difference between the direct inversion and LU schemes. Therefore, it seems reasonable to use the norm of the amplification factor defined as this difference to examine the AF error.

$$NAF - AF = \left\{ \frac{1}{2\,nmax} \sum_{i=1}^{nmax} \sum_{j=1}^{nmax} \left[\left| G_{ij,direct}\left(CFL, AR, \theta\right) \right| - \left| G_{ij,LU}\left(CFL, AR, \theta\right) \right| \right]^2 \right\}^{1/2} \tag{23}$$

where $G_{ij,direct}$ and $G_{ij,LU}$ are the amplification factors of the direct inversion and LU schemes, respectively. As the value of the NAF-AF approaches machine zero, the AF error decreases and the performance of the LU scheme approximates that of the direct inversion scheme more closely.

The convergence rate of the direct inversion scheme for the Euler equations, as we have seen in chapter 3.1.2, is governed by a single parameter, *CFL/AR*, irrespective of the magnitude of flow angle. The AF error shows similar trend. In Fig. 4, the NAF-AF after the first sub-iteration is presented for the case of $\theta AR=10^0$, irrespective of the magnitude of flow angel. The figure also indicates that the AF error remains unchanged even for very large *CFL* numbers.

Next, the behavior of the AF error during subsequent sub-iteration can be represented by the spectral radius to indicate the relative convergence rate.

$$Spectral\ Radius = \lim_{k\to\infty}\left(\frac{NAF - AF\ at\ sub-iteration = k}{NAF - AF\ at\ sub-iteration = 1}\right)^{1/k-1} \qquad (24)$$

In Fig. 5, the spectral radii of the NAF-AF are presented. The results show that the spectral radii are similar for all aspect ratio grids for a fixed value of *CFL/AR*. Therefore, it is seen that the magnitude of the AF error can be made independent to the grid aspect ratios if the *CFL* number is chosen as *CFL/AR* for grids with different aspect ratio.

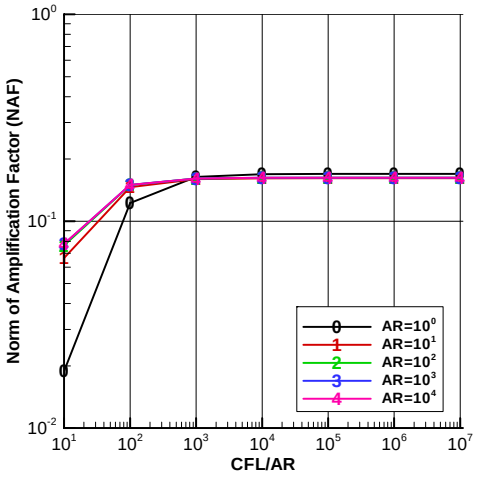

Fig. 4. Norms of Amplification Factor(NAF) of the AF error after the first sub-iteration for the Euler equations with $\theta AR=10^0$.

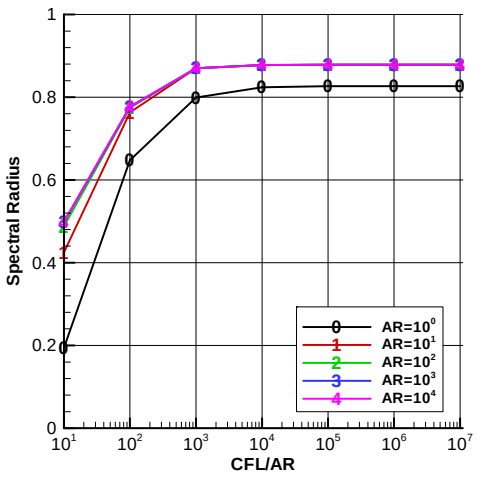

Fig. 5. Spectral Radius of the AF error during sub-iteration for the Euler equations with $\theta AR=10^0$.

4. Numerical Results

4.1 Uniform flow with a pressure disturbance

The findings from the stability analyses are now investigated by considering the solution of the Euler equations for uniform flow in a straight domain. By varying the aspect ratios of the domain while maintaining a fixed grid size(101×101), the local grid aspect ratio is arbitrarily increased from unity to 1×10^4. The initial condition used for all calculations is uniform flow plus a 10% pressure perturbation at one point in the center of the domain and the freestream Mach number is 0.5. Fig. 6 presents the number of iterations required for the error norm to fall 10 orders of magnitude. It is seen that the convergence rate is approximately same for all aspect ratio grids for a fixed *CFL/AR*. Also, it is seen that the LU scheme does not suffer convergence deterioration at any grid aspect ratios if large *CFL* numbers are used.

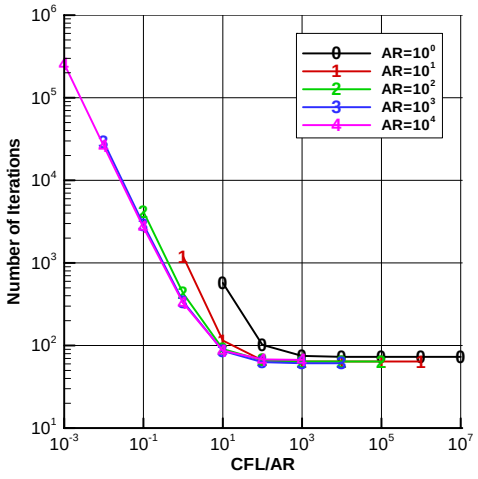

Fig. 6. Number of iterations to achieve 10 orders of error norm convergence.

5. Conclusions

A comprehensive study has been made for the investigation of the convergence characteristics of the LU scheme for the Euler equations using Von Neumann stability analysis. From the analysis of the scalar equation, it was found that the convergence rate is governed by a specific parameter

combination, which is *CFL/AR* for the case of large flow angle and *CFL×AR* for the case of small flow angle. Also, it was found that the convergence rate for the Euler equations is governed by only one parameter, *CFL/AR*, irrespective of the magnitude of flow angle. This suggests that if the local time step is defined based on *CFL/AR* for grids with different aspect ratios, the LU scheme for the Euler equations will not suffer convergence deterioration at any grid aspect ratios. The numerical results demonstrate that this time step definition gives uniform convergence for grid aspect ratios from one to million.

References

[1] Jameson, A. and Turkel, E., "Implicit Schemes and LU Decomposition", *Mathematics of Computation*, Vol. 37, No. 156, (1981), pp. 385-397.

[2] Strang, W. Z., Tomaro, R. F., and Grismer, M. J., "The Defining Methods of Cobalt$_{60}$: A Parallel, Implicit, Unstructured Euler/Navier-Stokes Flow Solver", *AIAA Paper*, 99-0786, Jan., (1999).

[3] Chen, R. F. and Wang, Z. J., "Fast, Block Lower-Upper Symmetric Gauss-Seidel Scheme for Arbitrary Grids", *AIAA Journal*, Vol. 38, No. 12, (2000), pp. 2238-2245.

[4] Jespersen, D. C., "Design and Implementation of a Multigrid Code for the Euler Equations", *Applied Mathematics and Computation*, Vol. 13, (1983), pp. 357-374.

[5] Buelow, P. E., "Convergence Enhancement of Euler and Navier-Stokes Algorithms", Ph. D. Thesis, The Pennsylvania State University, (1995).

[6] Anderson, W. K. and Bonhaus, D. L., "An Implicit Upwind Algorithm for Computing Turbulent Flows on Unstructured Grids", *Computers and Fluids*, Vol. 23, No. 1, (1994), pp. 1-21.

[7] Anderson, W. K., Thomas, J. L., and Van Leer B., "Comparison of Finite Volume Flux Vector Splittings for the Euler Equations", *AIAA Journal*, Vol. 24, No. 9, (1986), pp. 1453-1460.

[8] Whitfield, D. L and Taylor, L. K., "Discretized Newton-Relaxation Solution of High Resolution Flux-Difference Split Schemes", *AIAA Paper*, 91-1539, (1991).